Sādhanā (2021) 46:37
https://doi.org/10.1007/s12046-021-01558-8

Experimental analysis of low-temperature grain drying performance of vertical packed clay and clay-additives composite desiccant beds

C R HIREMATH[1,*] and KADOLI RAVIKIRAN[2]

[1]Department of Mechanical Engineering, BLDEA's V. P. Dr. P. G. Halakatti College of Engineering and Technology, Vijayapur 586103, India
[2]Department of Mechanical Engineering, National Institute of Technology Karnataka, Srinivasnagar, Mangalore 575025, India
e-mail: chandra.hiremath@yahoo.com; rkkadoli@nitk.edu.in

MS received 5 November 2019; revised 14 September 2020; accepted 17 December 2020

Abstract. A laboratory model of a forced circulation desiccant based green pea drying system operating in an open-loop is constructed and tested. The green pea drying process is divided into two stages involving dehumidification by the desiccant bed and green peas drying by dehumidified process air. Removal of moisture from the process air has been achieved by vertical packed composite desiccant beds. The composite desiccant used are heat treated clay with $CaCl_2$ being impregnated and clay with additives like horse dung and sawdust, again being heated, treated and later impregnated with $CaCl_2$. The green peas were dried for a process time of one hour. The drying was quite sharp during the initial process time of 500 s and from then onwards proceeded at a constant rate. For the identical bed masses, The performance of heat treated clay-additives based beds in moisture reduction and enhancement in enthalpy of process air is higher. The experimental study reveals the average heat content of air entering the dryer is 1.46, 2.46 and 2.38 kJ for heat-treated clay-$CaCl_2$, clay-horse dung-$CaCl_2$ and clay-sawdust-$CaCl_2$ composite desiccant beds of 700 g mass.

Keywords. Clay; additives; composite desiccant; dehumidification; heat content; drying.

1. Introduction

In developing countries, people are exploring the best possible ways of minimizing the post harvest loss of food products. The post-harvest losses are measured in terms of qualitative and quantitative losses. The control and minimization of qualitative losses in the form of calorific value, nutritional content and edibility, strengthens food security and improves the economy of the farming communities [1]. From the perspective of agricultural food product preservation, temperature and moisture content are the most important factors affecting the product quality during storage and aeration. Longer the storage of grains in wet ambient conditions causes mold growth. The control of deterioration of grain quality in humid tropical and subtropical countries is a significant task in grain aeration drying and cooling systems. Drying is a key process in post harvest technology applied to agricultural crops. Different drying techniques have been categorized as hot air and contact drying under atmospheric pressure, vacuum, freeze, infrared, super heated steam, impingement, solar, microwave and dielectric drying [2]. Energy equivalent to latent heat of vaporization is required to accomplish the transfer of moisture from the grains and then away from the grain surface. The driving force for the drying is the partial vapor pressure difference between the product surface and the surrounding process air. The warmer the process air more will be the moisture removed. Moisture removal from wet solid products brings about both volume and weight reduction. Thermal drying is a two stage process that involves transfer of heat from the surrounding environment to evaporate the exterior moisture and transfer of internal moisture to the surface of the solid and followed by its subsequent evaporation [3].

The common of drying technology suitable for rural farming areas are open air sun drying or solar drying. The employment of freely available solar energy for drying leads to inferior quality and spoilage of farm products. The traditional open air sun drying takes much of the time to dry agricultural yield and food products. However, the reasonable control of solar energy in drying is achieved by employing solar driers. The feasibility of an indirect natural convection stand alone solar dryer with thermal energy storage material for fruits and vegetables was investigated experimentally [4]. The drying process for grapes and green peas is accelerated by chemical pretreatment and with sand as thermal storage material. Experimental comparison of drying characteristics of pretreated green pea samples with

*For correspondence
Published online: 09 February 2021

untreated samples reveals the effect of pretreatments and drying temperature on drying time and rehydration capacity of the green pea drying process [5]. Though solar dryers provide suitable conditions for drying, the main disadvantage is the availability of solar energy during the daytime only. It is, therefore, advantageous to explore the periods during off sunshine hours. Continuous drying during day time and off sun shine hours is required to bring the moisture content to the desired level. Desiccant based drying systems provide the flexibility of drying during night time. The integration of continuous solar dryer with molecular sieve adsorbent and $CaCl_2$ absorbent for cocoa beans drying not only improves drying effectiveness but also reduces the drying time and specific energy consumption. During off sun shine hours, the humidity in the drying chamber is controlled by employing sorbents. The drying time as compared to conventional sun drying is reduced by 25% with molecular sieve solid adsorbent and by 45% with $CaCl_2$ liquid desiccant as thermal energy storage material [6].

In hot air driers with recirculation systems, the increase in relative humidity of process air after passing over the products decreases the moisture removal ability of process air. To enhance the prospective of process for drying it is useful to couple the recirculation driers with heat pumps, thermal storage materials and desiccants beds, so as to remove the extra moisture of the process air. The pair of recirculation dryer and desiccant system improves the overall drying efficiency of the system [7].

The condition of drying air affects the quality of the dried product in terms of nutritional loss, texture and color change. For example, products like mushrooms are sensitive when temperature of drying air is high. Higher temperatures and higher humidity of drying air also affect the color of drying product. Desiccant based drying systems are advantageous when drying requires low temperature and low humidity. The low temperature and low humidity of solid desiccant drying systems ensures good quality of wheat grains [8]. The desiccant materials have limited capacity to take moisture from air. The desiccants require regeneration for moisture removal. The use of solar and waste heat for regeneration of desiccants proves to be economical for drying. The integration of dryer with low temperature regenerated desiccant bed results in a compound dryer. Thermally regenerated desiccant systems with dryer are useful in the preservation and aeration of stored grains below atmospheric temperatures. The bentonite-$CaCl_2$ composite desiccant aeration system for the preservation of stored grain in humid climates employs solar energy for regeneration [9]. The experimental and theoretical analyses of forced convection desiccant integrated solar dryer for green peas drying under prevailing hot and humid atmospheric conditions of Chennai, India demonstrates the feasibility of drying during off sunshine hours. The quality of dried products improves and the characteristics of the desiccant remain stable even after a year [10]. A low temperature desiccant based food drying system with controlled airflow and temperature consists of rotary silica gel desiccant dehumidifier and drying chamber. The product dried by this method qualitatively reveals the sustainment of color and preservation of vitamin content as that of fresh vegetables. The drying system developed achieved higher drying speed than by sun drying [11]. The numerical simulation of the operational and physical parameters of the silica gel adsorption unit coupled with solar collectors and the dryer justifies the economy of drying apricots. The numerical simulations of theoretical model predict the temperature and moisture content of paddy under various aeration conditions. Numerically simulated results could lead to the development of appropriate practical systems for keeping grains not too dry or wet [12, 13].

The desiccant based systems employ liquid, solid, composite, polymer and bio desiccants in packed, radial, wheel, fluidized and annular bed configurations [14–17]. Compared to solid desiccants, liquid desiccants require lower regeneration temperatures and have higher moisture absorption capacities [18]. The use of solid desiccants requires higher regeneration temperature and the use of liquid desiccants requires continuous recirculation. In order to have the best features of solid and liquid desiccants, the impregnation of liquid desiccants with solid desiccants leads to composite desiccants for moisture adsorption. Clay being the natural material and the impregnation of $CaCl_2$ with clay produces clay based composite desiccants that have potential application in drying and aeration of food products [19, 20].

The literature study reveals the use and importance of desiccant materials in food products preservation and drying. Implementation of desiccants in a drying system is becoming an attractive alternative for food grain preservation and drying. Desiccant dehumidification units integrated with drying and aeration systems controls the process air humidity and reduces the latent load of the system. The other advantages of desiccant dehumidification systems such as low initial operating costs, lower drying time, environmental friendliness, low drying temperatures and significant potential for energy savings where low grade solar thermal heat energy is employed for regeneration.

The above studies show that desiccant assisted drying systems are one of the best drying method. The current work deal with laboratory scale grain dryer integrated with vertical packed clay-$CaCl_2$ and clay-additives-$CaCl_2$ composite desiccants. The main objective is to study the potential of clay based composite desiccants in drying green peas agriculture produce in terms of moisture reduction, enthalpy and drying rate of process air. The present study identifies locally available natural materials like transported clay (referred to as clay in short), additives like sawdust and horse dung in preparation of clay composite desiccants. Experiments are conducted to evaluate the effect of desiccant bed inlet air temperature, relative humidity and bed mass on dehumidification and grain drying performance of process air.

2. Methodology

The methodology includes manual preparation of clay and clay-additives based $CaCl_2$ composite desiccants. Construction and setting the desiccant based system for green pea (*Pisum sativum*) drying. The fresh good quality green peas purchased from a local dairy for drying experiments. Instrumentation employed for the measurement of properties of process air, desiccant bed and grain drier parameters.

2.1 *Preparation of clay and clay-additives composite desiccants*

The materials employed for the preparation of clay based composite desiccants are naturally available transported clay, additives like sawdust and horse dung and 50% $CaCl_2$ solution. The liquid desiccant carrier, namely the transported clay, is available in banks and bed of the lake, located in Vijayapur district of Karnataka state, India. The transported clay in the clinker form was collected from the pot maker. The collected clay is then crushed and ground to obtain the powdered clay material. It has been an age old practice in the local region of Vijayapur that the horse dung is mixed with transported clay while preparing earthen ware. It is their intuition and experience that horse dung when added to transported clay imparts strength and porosity to the earthen wares produced. Sawdust a residue of saw mill is employed as another additive. The additives are mixed separately with clay in the proportion of 20% by weight. The pasty clay and clay-additives material is obtained by adding required quantity of water. The green clay and clay additives materials are manually molded to the spherical shape of 10 mm diameter. The spherical shaped clay and clay with additives are dried at room temperature. Subsequently, they are heat-treated to 500°C.

The heat treatment of clay-additives samples in furnace is in presence of oxygen. During heat treatment either the horse dung or sawdust being additives in the clay gets oxidized. Complete oxidation will induce porosity or will be retained as carbon in clay samples. The result of the heat treatment of the clay-additives spherical balls will destroy the obnoxious character of the horse dung. Additives horse dung or sawdust will be in the form of carbon in the clay mixture. The heat treated clay and clay-additives composite desiccants are then impregnated with $CaCl_2$ liquid desiccant of 50% concentration. The higher porosity in clay additives desiccants helps to retain higher quantity of $CaCl_2$ and thereby enhances dehumidification capacity. Thus the three composite desiccants namely clay-50% $CaCl_2$, clay-20% sawdust-50% $CaCl_2$ and clay-20% horse dung-50% $CaCl_2$ are produced. The manually prepared composite desiccants are finally kept in airtight plastic boxes. The SEM images were taken under 5000X magnification for heat-treated clay and clay-additives composite desiccants before impregnation and after impregnation are presented in figures 1(a) to (e). The surface texture of SEM images reveals an uneven surface comprising long voids. The scattered white regions of varying sizes (figure 1(c) and (e)) indicate the dispersion and concentration of sawdust and horse dung with clay. The dense white patches corresponding to impregnated burnt clay and burnt clay-additives. Figures 1(b), (d) and (f) reveal the deposition of $CaCl_2$ layers onto the surface of heat treated clay and clay-additives composite desiccants.

2.2 *Analysis of water uptake by the clay and clay-additives composite desiccants*

In order to ascertain the hygroscopic property of composite desiccants, few samples of desiccants are picked from the lot and are exposed to the atmosphere. The photographs of clay and clay-additive composite desiccant are shown in figure 2. Visual observation reveals that the surface of the clay and clay-additives impregnated with $CaCl_2$ desiccant has become wet. It can be inferred that the transfer of moisture on to the desiccant surface and into the desiccants has taken place by convective and diffusive transport. The test shows the hyperactivity of some desiccants towards moisture adsorption. On the other hand, there is a time lag towards adsorptivity of remaining desiccants. The test on clay and clay-additives desiccants reveals the non-uniform dehumidification behavior of clay and clay-additives based composite desiccants. This behavior may influence the heat and mass transfer characteristics of vertical packed clay composite desiccant beds.

Further, in order to investigate the relative dehumidification potential of clay composite desiccants, tests have been conducted wherein desiccants are exposed to the controlled condition of process air. The experiments are conducted by keeping the desiccant particle in temperature controlled humidity chamber. The water uptake is calculated as the difference between by the initial mass of desiccant and the mass of the desiccant at a particular time during adsorption. Figures 3(a) to (d) depict the time variation of water uptake by desiccants at 45°C and exposed to humidity conditions of 24%, 34%, 42% and 52%. For the process air relative humidity of 24% and 34%, the trends for water uptake by desiccants is alike and proceeds coincidentally with each other. The qualitative behavior of moisture adsorption by desiccants spans even after one hour of process. From then onwards, the water content monotonously increases for clay-additives based desiccants, whereas for clay based desiccant tending

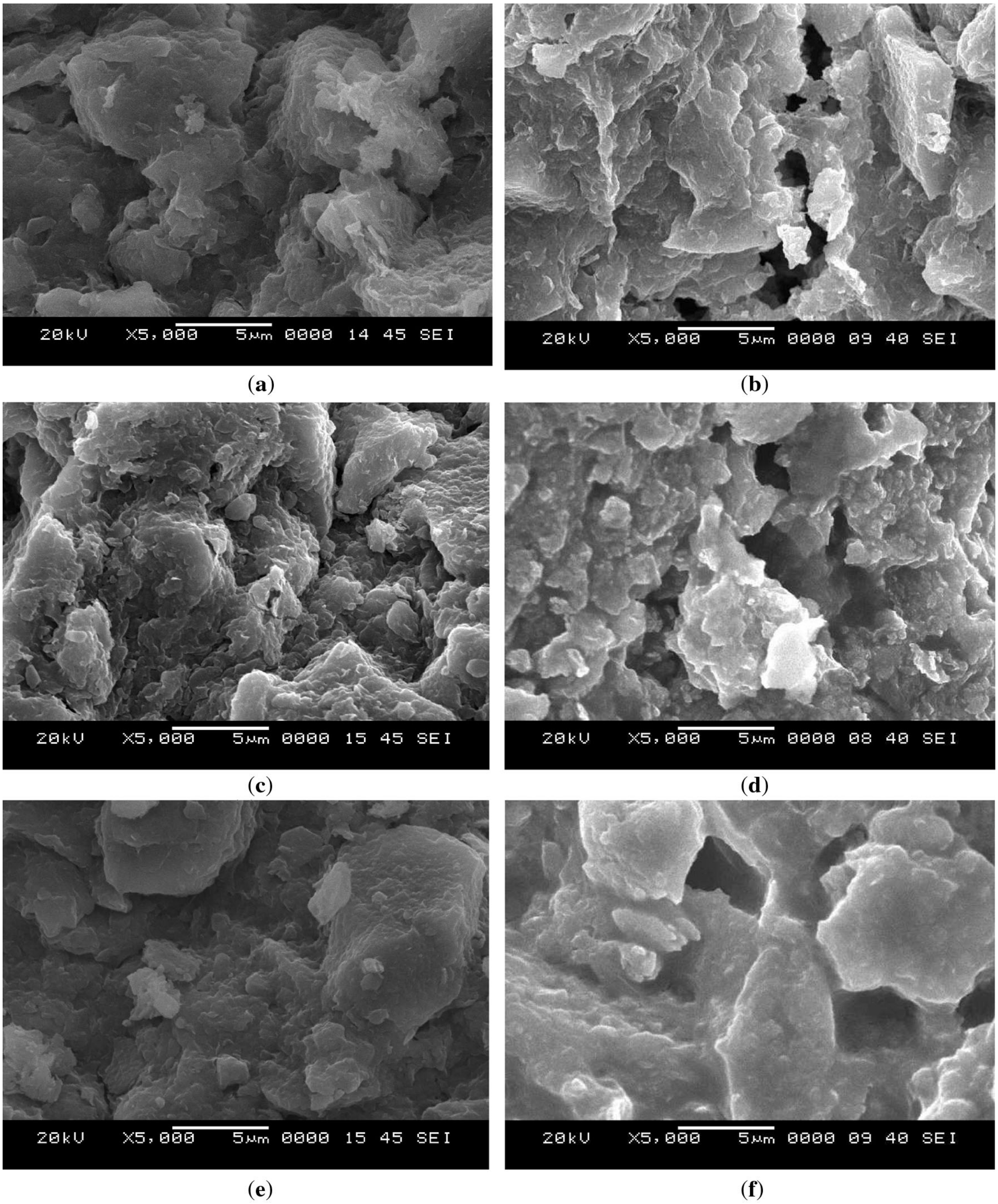

Figure 1. SEM micrographs of heat treated (a) clay, (b) clay-50% $CaCl_2$, (c) clay-20% horse dung, (d) clay-20% horse dung-50% $CaCl_2$, (e) clay-20% sawdust and (f) clay-20% sawdust-50% $CaCl_2$ composite desiccants.

towards saturation. For the relative humidity of 42% and 52%, the water content of composite desiccants increases nearly in equal proportion. The concentration of moisture shared by the desiccants seems to be nearly the same up to the process time of half an hour. Beyond that time span, the water content of composite desiccants is scaled up till near to the saturation. From the results, it reveals that the burnt clay-$CaCl_2$ composite desiccant saturated with the water content. As compared to clay-additives desiccants attainment of saturation condition is at accelerated rates for burnt clay-$CaCl_2$ desiccant. As compared to clay composite desiccant the moisture uptake rate is higher for clay-additives based composite desiccants and adsorption process continues till the beds are saturated.

Figure 4 depicts water content of clay and clay additives composite desiccants with different humidity conditions of

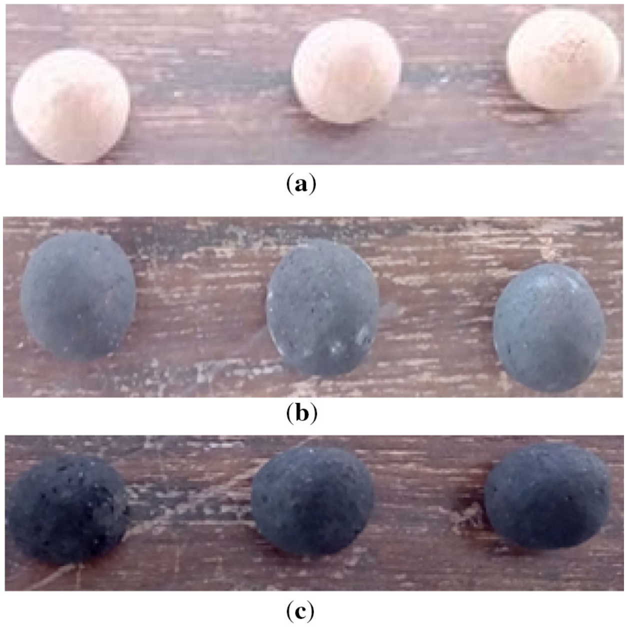

Figure 2. Photographs showing samples of heat treated (a) clay-50% $CaCl_2$, (b) clay-20% saw dust-50% $CaCl_2$ and (c) clay-20% horse dung-50% $CaCl_2$ composite desiccants.

process air at 45°C such as 24%, 34%, 42% and 52%. For all the tests the duration of adsorption time is fixed to about 4 hours. From the results, it is observed that at higher relative humidity, higher will be the water content of clay and clay-additives based composite desiccants. Irrespective of process air humidity levels and for identical exposure time, burnt clay-horse dung-$CaCl_2$ composite desiccant exhibit higher rates of moisture uptake. Clay-additives composite desiccants are capable of holding large quantity of water due to presence of higher mass of $CaCl_2$ into the pores. The presence of higher mass of $CaCl_2$ is evident from the SEM images as presented in figures 1(b), (d) and (f) with impregnated clay-additives desiccants is due to the porous and uneven surface texture.

2.3 *Construction and arrangement of an experimental set-up*

The experimental se-tup consists of mainly the reciprocating air compressor (1), vertical acrylic tube as a desiccant bed (3), drying chamber (4) consists trays (T1 and T2) and instrumentation. The reciprocating air compressor has a rating of 2.2 kW with a free air delivery up to 15 m^3/h. The vertical acrylic tube has, 0.054 m and 0.05 m as outside diameter and inside diameter respectively, and length being 0.07 m for containing the desiccants. The schematic of the experimental set-up is shown in figure 5(a). A perforated sheet is provided at the bottom end of the tube that enables to hold the desiccant particles. Prototype drying cabinet of dimensions 0.43 m × 0.41 m × 0.54 m (Length × Width × Height) is fabricated from 19 mm thick mild steel sheets. The drying trays are made using wire mesh placed inside the drying chamber with dimensions of 0.31 × 0.31 m^2 to hold the green pea grains which will be subjected to drying. The diameter of perforated holes is 0.0003 m and the holes are arranged at a pitch of 0.007 m along with vertical and horizontal directions. The distance between the two trays is 0.10 m. The bottom tray (T1) is at a distance of 0.45 m from the dryer inlet. The distance between the top tray (T2) and the exit of the dryer is 0.27 m. The air flows vertically through the grain samples. The drying trays can be easily removed to load and unload the drying products from the door, which is provided on the front side of the drying chamber. At the top of the drying chamber, an air gap of 0.12 m is provided with a GI pipe that exits humid air to the atmosphere. Manually operated gate and ball valves (V1 to V10) are provided to regulate the process airflow. The airflow diagram of the drying system is shown in figure 5(b) wherein the compressed air is ducted to the drying chamber through the desiccant bed. The warm dehumidified air leaving the desiccant bed transfers its sensible heat to the grains on the trays and finally leaves at the top of drying cabinet to atmosphere under forced circulation mode.

Drying experiments are carried out to study the green pea dryer performance with three vertical packed composite desiccant beds. (a) Dryer coupled with burnt clay-50% $CaCl_2$ desiccant bed, (b) dryer coupled with burnt clay-20% sawdust-50% $CaCl_2$ desiccant bed and (c) dryer coupled with burnt clay-20% horse dung-50% $CaCl_2$ desiccant bed. The relative humidity and temperature of process air at desiccant bed inlet (H1), exit (H2) and dryer exit (H3) were measured using a Rotronic hygroflex humidity sensor. The humidity sensor has a 0 to 100% range on relative humidity and -40 to 85°C range on temperature. The accuracy of the instrument for RH is ±1% and for temperature, it is ±0.2°C. A microcontroller board (arduino) is employed to interface the humidity sensors to the computer (5). The voltage values corresponding to relative humidity and temperature are written to a text file for every second with the execution of microcontroller code. K-type (Chromel-Alumel) thermocouples are used to measure the desiccant bed temperature at four positions along the axial direction of the bed. The first thermocouple is located at a distance of 0.06 m from the desiccant bed inlet. The axial distance between the thermocouples is 0.08 m along the vertical tube. The temperature inside the drying chamber is measured using another two K-type thermocouples. Desiccant bed and dryer temperature measurement locations are shown by the filled star symbol as shown in figure 5(a). The temperatures are recorded every 300 s of process. The pressure drop across orifice meter and through the desiccant bed and the dryer are measured by water filled U-tube manometers (M1, M2, and M3). The moisture content of desiccant bed and green pea grains before and after the process are measured using an electronic balance of range 0.2 to 300 g with accuracy of 0.01 g. The mass flow rate of

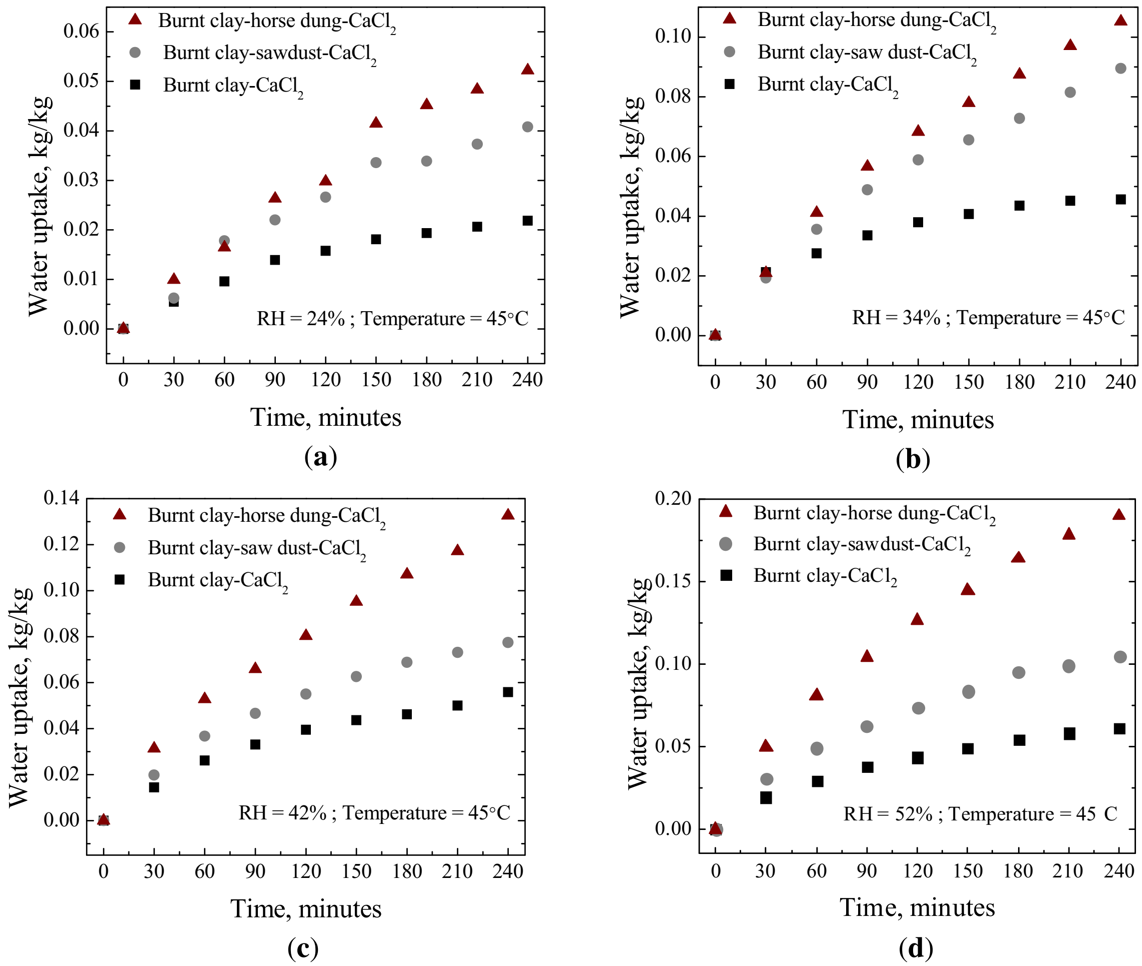

Figure 3. Transient variation of water uptake capacity for heat treated clay-additives-$CaCl_2$ desiccants in adsorption.

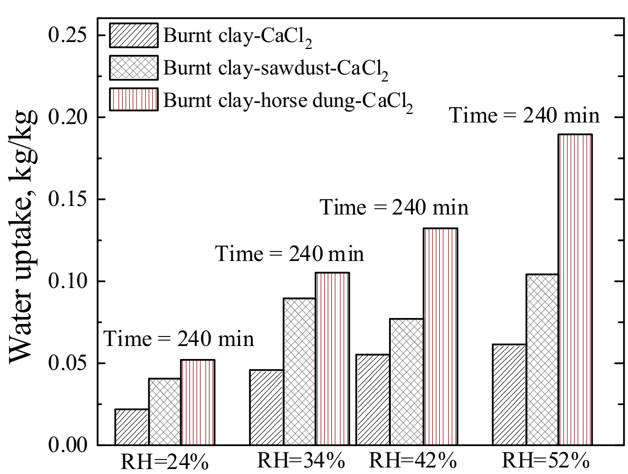

Figure 4. Variation of water content for heat treated clay-additives-$CaCl_2$ composite desiccants in adsorption.

process air is measured using calibrated orifice-meter (2) of 0.01 m diameter and coefficient of discharge as 0.68. Experimental runs were conducted for 500 g of green pea with a maximum 750 g of desiccant bed mass. The uncertainties of the measured parameters are estimated according to the methods given in references [21, 22] and are listed in table 1.

2.4 *Process air, desiccant bed and grain dryer performance indices*

In estimating the performance parameters, the pipe losses are neglected. The moisture reduced from the process air by the desiccant bed (m_{db}) and moisture transported to the process air from the moist grains (m_{gb}) in the dryer is calculated on a wet basis of process air are given by non dimensional Eqs. (1) and (2).

$$m_{db} = \left(\frac{W_{a_i} - W_{a_e}}{W_{a_i}}\right) \times 100 \tag{1}$$

$$m_{gb} = \left(\frac{W_{a_e} - W_{a_i}}{W_{a_e}}\right) \times 100 \tag{2}$$

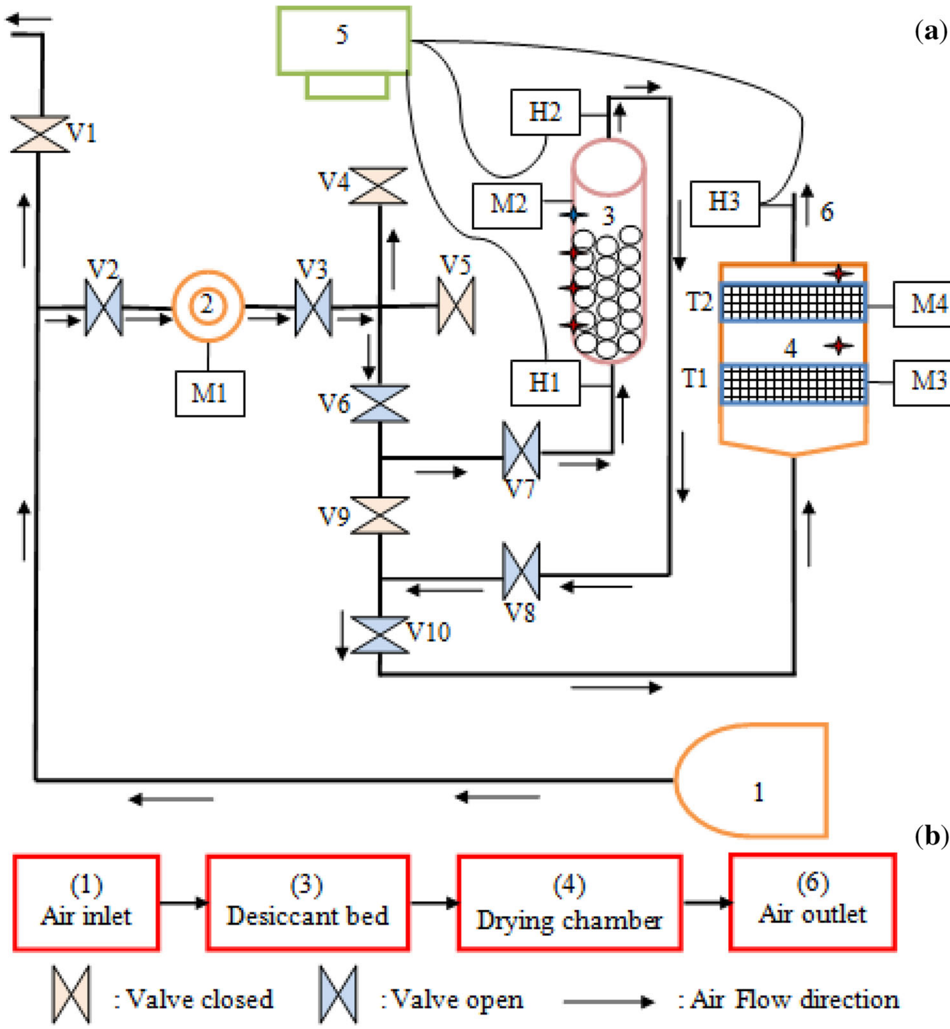

Figure 5. Schematic view of (a) desiccant bed coupled with grain dryer and (b) air flow diagram.

Table 1. Uncertainties in the measurement of experimental parameters.

Process air humidity ratio	$\pm\sqrt{\left(\frac{\partial W}{\partial P_v}\right)^2 \times \left(\left(\left(\frac{\partial P_v}{\partial RH}\right)^2 \times (\omega RH)^2\right) + \left(\left(\frac{\partial P_v}{\partial P_{sat}}\right)^2 \times (\omega P_{sat})^2\right)\right)} = \pm 1.39\%$
Process air velocity	$\pm\sqrt{\left(\frac{\partial v}{\partial X}\right)^2 \times (\omega X)^2} = \pm 0.40\%$
Mass of sample	$\pm\frac{\partial w_g}{w_g} = \pm 0.004\%$

The amount of surface area (A_{sf}) available for the given volume of bed and porosities (ε_b) for moisture and heat transfer in the clay and clay-additives composite desiccant beds [23] are estimated using the following equations (Eqs. (3) and (4))

$$A_{sf} = \frac{6(1-\varepsilon_b)}{(d_P)} \times (V_b) \tag{3}$$

$$\varepsilon_b = 1 - \left(\frac{\rho_b}{\rho_d}\right) \tag{4}$$

Equation (5) represented the absolute enthalpy (h_a) which is a function of humidity ratio and temperature of process air at desiccant bed inlet and exit [24]. The instantaneous drying rate (dr) on dry basis of process air in drying the grains is computed using Eq. (6). The overall moisture removed from the grains (Mr) is defined as the ratio of reduction in grain mass (G) which is the difference in the mass of grains before and after the drying process to the total drying time (t_d) of 60 minutes is expressed by Eq. (7).

$$h_a = (1005.22 + 0.02615T_a)T_a + (W_a/1000) \times (2500800 + 1868T_a) \quad (5)$$

$$\mathrm{d}r = \frac{W_{a_t} - W_{a_{t+dt}}}{dt} \quad (6)$$

$$Mr = \frac{G}{t_d} \quad (7)$$

Table 2 details the experimental parameters for the dryer with clay-based $CaCl_2$ composite desiccant beds. From table 2, it is clear that for the same bed masses, the bed surface area available for moisture transport for clay-additives based composite desiccant beds is higher as compared to clay-based composite desiccant beds. The increase in the surface is due to higher bed volumes per unit mass of desiccant bed. For the same bed masses, a higher length of bed that prevails in additive based desiccant beds results in higher surface area. Higher the bed masses higher will be the pressure drop through the clay and clay-additives composite desiccant beds. For the same bed diameter to length (D/L) ratio of 0.18, the pressure drop through the vertical packed clay additives beds is 16% lower than vertical packed clay-based desiccant beds. The porosities estimated using Eq. (4) for clay-$CaCl_2$, clay-horse dung-$CaCl_2$ and clay-sawdust-$CaCl_2$ composite desiccant beds are 0.70, 0.86 and 0.87. The higher bed porosities are prevailing in clay-additives composite desiccant beds result in a lower pressure drop. As humid air comes in contact with the dry desiccant bed and due to vapor pressure difference, process air transfers its moisture content to clay and clay additives composite desiccant bed. The dehumidification by desiccant releases heat of adsorption that increases the bed temperature and subsequently raises the temperature of process air. The warm dehumidified air exiting the desiccant bed is conveyed into the dryer containing grains on the bottom and top trays. The higher enthalpy content of air removes more moisture from the grains contained in the bottom tray. The amount of moisture removed from the grains contained in the bottom tray is higher than the grains contained in the top tray.

3. Results and discussion

Experiments are conducted to determine the effectiveness of proposed clay additives composite desiccants for drying of green pea grains. The experimental runs for differing desiccant bed mass (300 g to 700 g) are conducted. The velocity of air at the inlet of desiccant bed was 1.5 m/s. The

Table 2. Experimental conditions and results for dryer coupled with clay and clay-additives-$CaCl_2$ composite desiccant bed.

	Composite desiccant bed parameters					Grain dryer		
						Moisture removed (% Wet basis)		
Type of bed	Bed mass (g)	D/L ratio	Surface area (m^2)	Pressure drop (mm of water column)	Weight gain (% Wet basis)	Tray - T1	Tray - T2	Exp Runs
Burnt clay-$CaCl_2$	300	0.40	0.045	20	1.31	12.91	10.75	R1
	500	0.19	0.085	35	1.82	6.26	4.32	R2
	550	0.19	0.094	38	1.18	9.89	3.44	R3
	600	0.18	0.097	38	1.68	10.02	6.78	R4
	650	0.16	0.112	40	1.63	7.39	5.02	R5
	700	0.15	0.117	49	1.28	6.76	8.33	R6
Burnt clay-horse dung-$CaCl_2$	300	0.23	0.061	22	4.50	9.79	7.23	R7
	350	0.21	0.067	28	3.68	7.21	5.18	R8
	400	0.18	0.076	31	3.75	10.05	6.59	R9
	450	0.16	0.083	38	4.58	9.89	4.80	R10
	500	0.15	0.091	40	1.64	11.71	6.66	R11
	700	0.10	0.135	48	1.35	10.63	8.69	R12
Burnt clay-sawdust-$CaCl_2$	300	0.22	0.063	25	2.33	4.66	4.54	R13
	350	0.21	0.067	28	3.28	10.54	7.26	R14
	400	0.18	0.076	32	2.99	9.72	6.35	R15
	450	0.16	0.086	39	3.04	8.83	7.22	R16
	500	0.15	0.091	40	2.47	12.05	9.44	R17
	700	0.10	0.132	53	2.84	7.35	4.92	R18

experimental parameters estimated for different runs are presented in table 2.

3.1 *Analysis of process air parameters for heat treated clay and clay-additives-$CaCl_2$ composite desiccant beds and grain dryer*

Figures 6(a) and (b) show the comparison of transient variation of air moisture reduction from process air and enthalpy of process air entering into the dryer. Air moisture reduction is estimated using Eq. (1) and absolute enthalpy of air exiting the desiccant bed is calculated using Eq. (5). For the same bed masses, higher moisture reduction rates are noted for clay-additives-$CaCl_2$ composite desiccant beds. For the identical desiccant bed masses of 700 g, bed length of 0.33 m and 0.50 m are noted for clay-$CaCl_2$ and clay-additive-$CaCl_2$ composite desiccant beds, respectively. The higher bed length of clay additives desiccant beds enables more bed surface area for process air dehumidification. The higher bed length per unit volume of bed offers higher residence time for the air to pass through the interstitial spaces of bed. As presented in figure 6(a) for the process time below 250 s, moisture reduction increases up to 60% for clay-additives based desiccant beds. With progress in process time the desiccant bed water content increase which in turn progressively decreases moisture uptake capacity of the bed. The transient variation of enthalpy of air exiting the desiccant bed and entering into the dryer is shown in figure 6(b). For the beds having a higher surface area, higher will be the moisture adsorptivity. Higher dehumidification potential of additives desiccant beds, releases higher heat of adsorption. Due to this the bed temperature increases and subsequently increases the temperature of air leaving the desiccant bed.

For the same D/L (bed diameter to bed length) ratio of 0.16, the transient variation of moisture reduction and enthalpy of air are graphically presented in figures 7(a) and (b). As compared to clay-based desiccant bed, additive based desiccant beds show slightly higher adsorptivity. The peak values of moisture reduction and heat content are observed within 250 s of process time. From then onwards the increase in bed water content decreases vapor pressure difference between the desiccant surface and the

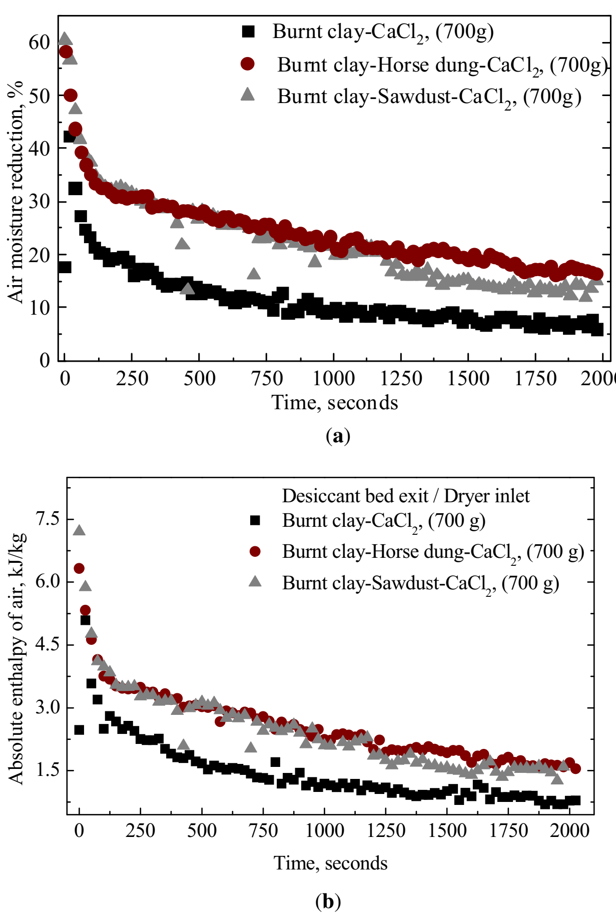

Figure 6. Transient variation of (a) moisture reduction and (b) enthalpy of process air for experimental runs R6, R12 and R18.

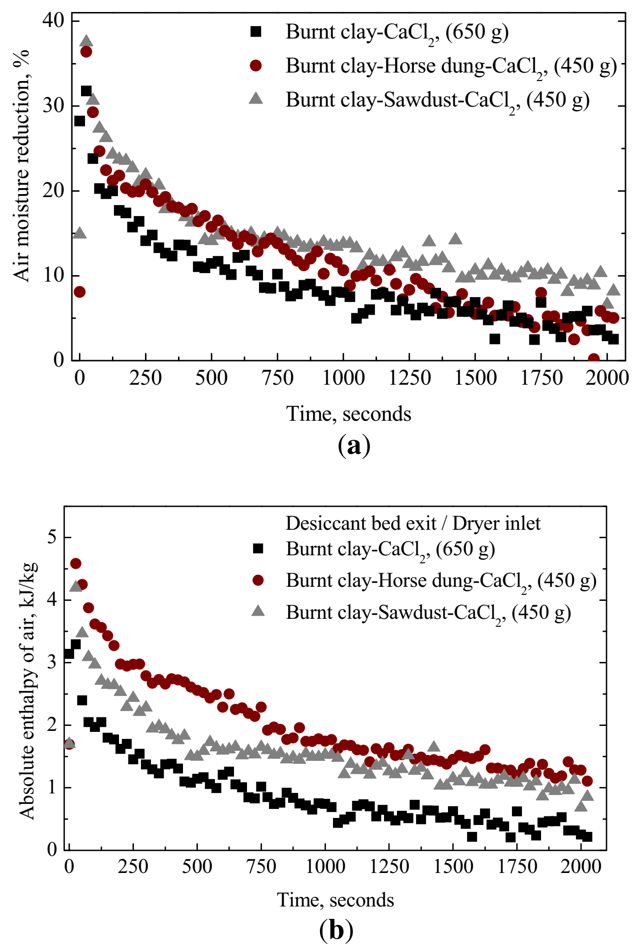

Figure 7. Transient variation of (a) moisture reduction and (b) enthalpy content of process air for experimental runs R5, R10 and R16.

surrounding air. The increase in vapor pressure on desiccant surface progressively decreases the adsorption rate which in turn counteracts the adsorption heat and bed temperature decreases. Lower adsorptivity with progress in time reduces the enthalpy of air. From the results of the same bed masses (figure 6(b)) and similar D/L ratios (figure 7(b)) it is observed that enthalpy levels of process air exiting the desiccant bed are higher in clay-additives based composite desiccants. As compared to D/L ratio, process air moisture reduction and humidity reduction are high when identical desiccant bed masses are considered. For the same bed masses, the numbers of desiccants contained in the vertical bed are more in clay-additive composite desiccant beds. The lesser density of additives desiccants enables higher bed length that enables higher bed surface area for moisture reduction. The higher number of desiccants for the same cross-section area of bed yields higher bed adsorptivity.

The net moisture reduced and net enthalpy added to process air is functions of desiccant bed inlet and exit air relative humidity and temperature. The net moisture and enthalpy transferred are evaluated by using desiccant bed inlet and exit air humidity ratio and enthalpy. The transient variation in net moisture content of process air transferred to the desiccant bed and net enthalpy added to process air by the desiccant bed in adsorption are illustrated in figures 8 (a) and (b). The results are compared for the same D/L ratio of 0.18. During the initial period of adsorption the higher decrease in net air humidity ratio indicated a higher potential of clay and clay additives composite desiccant beds towards moisture adsorption. The adsorption heat released during the initial period of operation results in higher heat transferred to process air from the desiccant beds. With the advancement in time moisture transferred to the bed and heat transferred to the air decreases.

Process time variation of exit air humidity ratio and temperature with respect to inlet air humidity ratio and temperature for desiccant beds and grain dryer are depicted in figures 9(a) to (f). The process air having average specific humidity of 4.66, 4.4, 4.32 g of water vapor/kg of dry air and temperature of 23.02, 21.57, 20.30°C is introduced into the vertical packed burnt clay-$CaCl_2$, burnt clay-horse dung-$CaCl_2$ and burnt clay-sawdust-$CaCl_2$ composite desiccant bed mass of 550 g, 400 g and 700 g. The superficial velocity of air is 1.5 m/s. Within the process time of 500 s, the process air experiences maximum reduction in its moisture content. From 500 s onwards, the process of adsorption weakens and moisture uptake capacity of bed decreases and subsequently the exit air humidity ratio nears the bed inlet air humidity ratio. As the process of adsorption in early stages is high enough to increase the bed temperatures and subsequently increases the exit temperatures of air. The effect of the heat of adsorption is significant within 500 s. The heat of adsorption which reflects the enthalpy variation before and after adsorption is calculated using Clausius-Clayperon equation

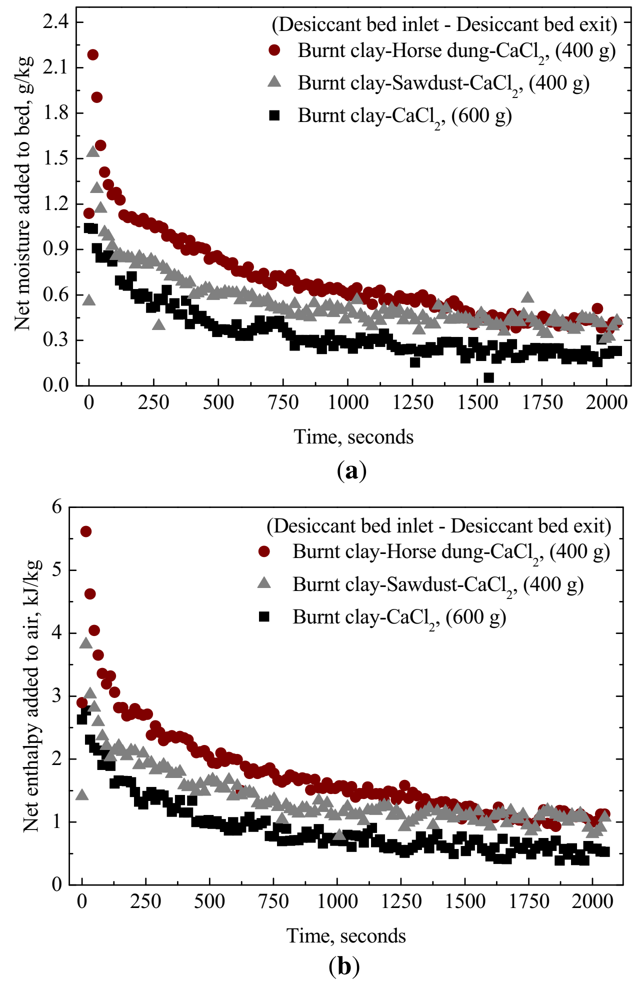

Figure 8. Variation of net (a) moisture added to bed and (b) enthalpy added to process air with time for experimental runs: R4, R9 and R15.

[25]. The average bed temperatures measured for 550 g burnt clay-$CaCl_2$, 400 g burnt clay-horse dung-$CaCl_2$ and 700 g burnt clay-sawdust-$CaCl_2$ are 30.48, 31.65 and 31.07°C. The desiccant bed enthalpy variation in terms of heat adsorption estimated are 28.97, 29.04 and 29.05 kJ/kg for the respective clay and clay-additives composite desiccant bed average temperatures. The average heat content of air entering the dryer is 1.46, 2.46 and 2.38 kJ for heat-treated clay-$CaCl_2$, clay-horse dung-$CaCl_2$ and clay-sawdust-$CaCl_2$ composite desiccant beds of 700 g mass.

The warm dehumidified air exiting the clay composite desiccant beds is conveyed into the grain dryer. The warm dehumidified air comes in contact with the wet grains which are spread on the trays of the dryer. The heat energy transferred to grains extracts moisture and then exits the dryer with higher humidity and lower temperature levels. Owing to heat of adsorption in the early stage of the process, moisture removal from the grains is more significant in the early stage of drying. The process air after drying leaves the dryer at higher humidity levels than desiccant

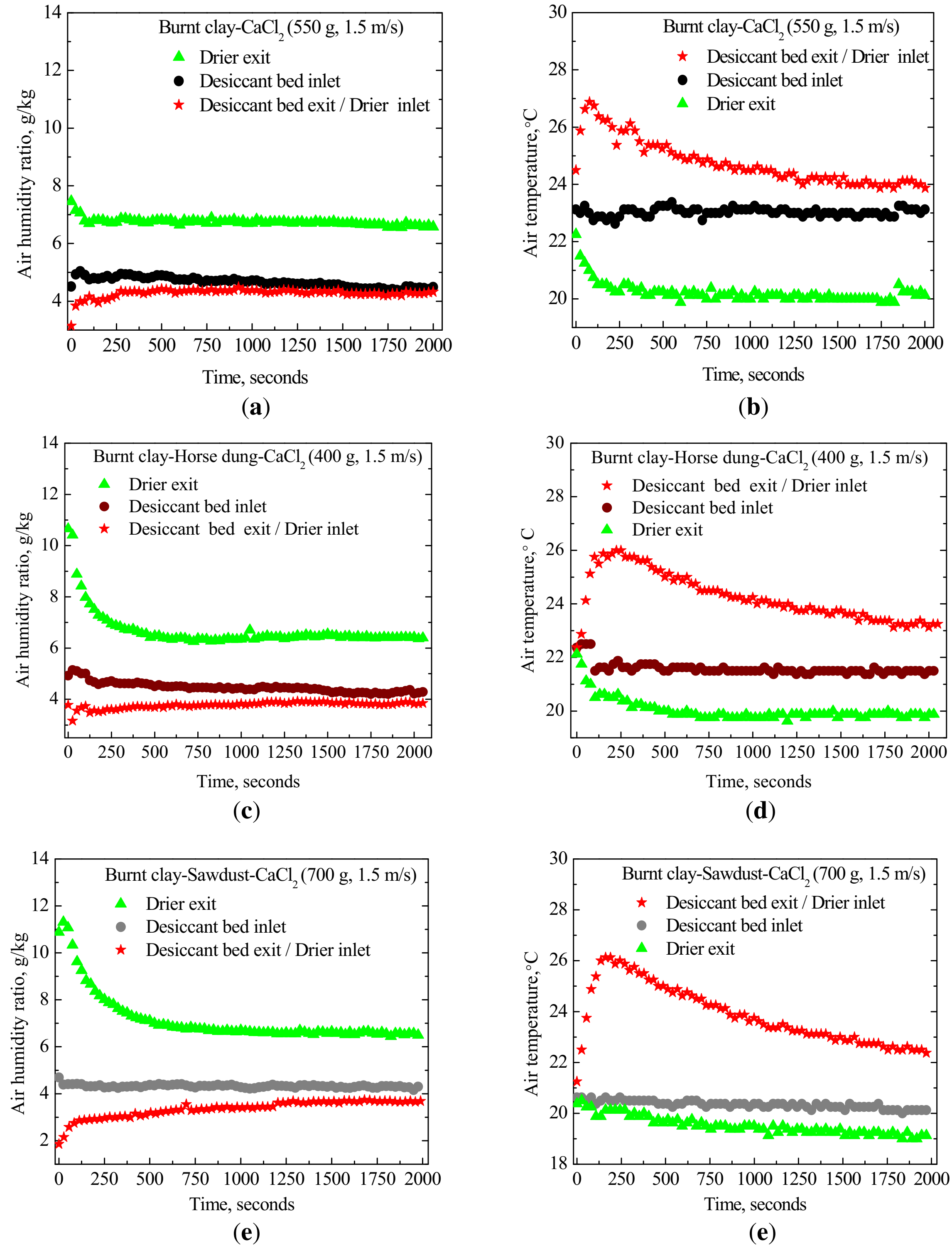

Figure 9. Variation of desiccant bed and dryer exit air humidity ratio and temperature with time for experimental runs R3 (a, b), R9 (c, d) and R18 (e, f).

bed inlet air humidity levels. The temperatures of air leaving the dryer are lower than the desiccant bed inlet air temperatures. The total water content removed from the grains contained on the bottom and top trays are 13.33 g, 16.64 g and 12.27 g for vertical packed 550 g burnt clay-$CaCl_2$, 400 g burnt clay-horse dung-$CaCl_2$ and 700 g burnt clay-sawdust- $CaCl_2$ composite desiccants, respectively.

Transient variation of net moisture uptake from grain bed by drying air and moisture uptake by desiccant bed from the dehumidified process air is illustrated in figures 10(a),

(b) and (c). The moisture reduction of air is a function of desiccant bed inlet air relative humidity, temperature, bed mass, bed inlet air velocity and atmospheric conditions. Moisture uptake by air is a function of dryer inlet air humidity, temperature, mass flow rate, grain initial moisture content. During the initial period of adsorption the higher percentage of moisture removal by the desiccant bed results in higher moisture uptake from the grain samples and subsequently increases the dryer exit air moisture content. The maximum removal of moisture from the grains is of short duration (0 to 500 s) wherein grain surface moisture is likely to be removed. From 500 s onwards, moisture removal rate is steady wherein grain bound moisture gets removed. The minimum and maximum moisture content of air leaving the dryer within 500 s are 57.81% and 33.66% for 550 g bed mass. From 500 s onwards the moisture content of process air leaving the desiccant bed and dryer remains steady.

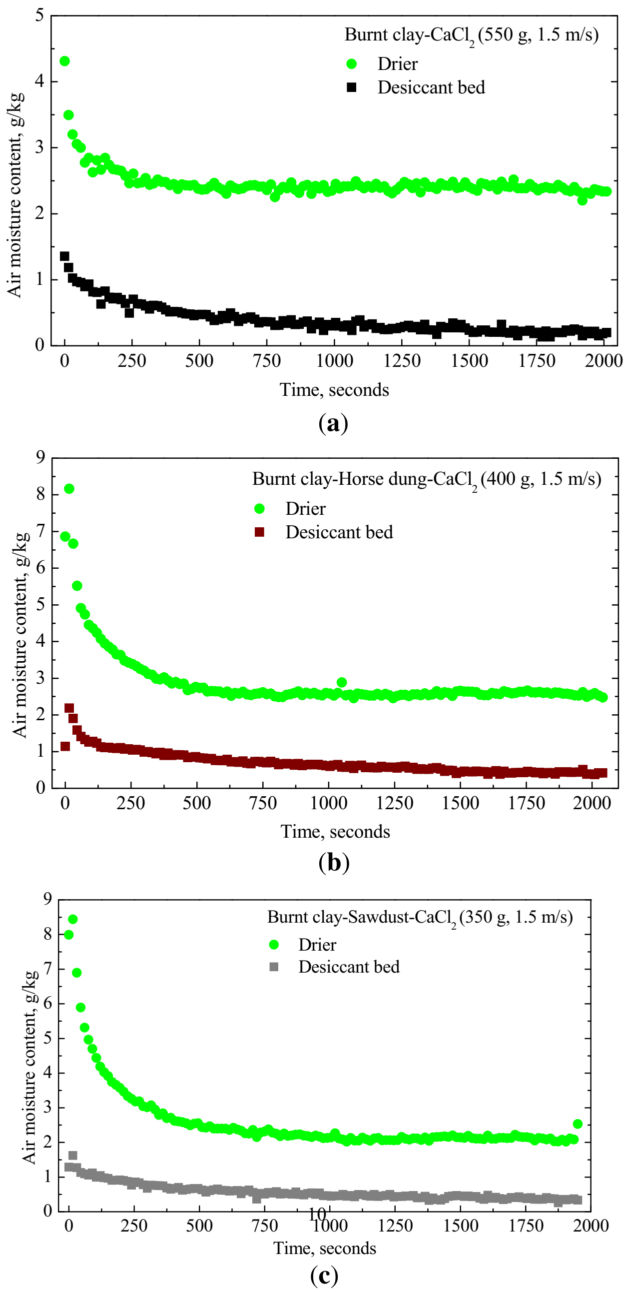

Figure 10. Time variation of moisture content of process air exiting the desiccant bed and grain dryer for experimental runs R3 (a), R9 (b) and R14 (c).

The transient variation of moisture content of air exiting the bed mass of 400 g burnt clay- horse dung-$CaCl_2$ desiccant bed and dryer is graphically presented in figure 10(b). The maximum reduction and gain in moisture by process air due to dry desiccant bed and moist grains during the entire process time are 44.23% and 74.58% for 400 g, bed masses. Within the period of 500 s, the average values of reduction and gain of moisture by process air are 23.88% and 50.34%.

The variation of air moisture content with time due to dehumidification and humidification by 350 g bed mass burnt clay-sawdust-$CaCl_2$ desiccant bed and dryer is shown in figure 10(c). During the initial period of 500 s, the average moisture content of process air through the desiccant bed and dryer are 20.15% and 50.24% for 350 g bed mass. At the end of the drying process, the dryer exit air moisture content decreases to a minimum value of 30.91%, for the respective bed masses of 350 g.

The drying rate for the process air exiting the dryer is estimated using Eq. (6). The graphical illustration of drying rate presented in figures 11(a) and (b) show the presence of three phases namely surface evaporation stage or external drying (0 to 100 s), migration of moisture within the grains to the surface or internal drying (100 to 500 s) and constant rate drying (from 500 s onwards). The surface evaporation phase and diffusion of moisture within the grains to surface spans from 0 to 500 s of process time and from then onwards drying proceeds at steady rate. In the surface evaporation phase, higher drying rates are noticed. Heat is transferred to the surface of wet green peas (or undried green peas, or dampened green peas or moist laden green peas). The warm dehumidified air easily evaporates the green pea food product water. The humidity of air increases at approximately constant enthalpy, neglecting the heat losses to the surroundings. The removal of moisture from the grains in first phase is function of circulating air temperature, humidity, flow rate and surface area of the green peas. In the second phase the drying rate is falling and progresses with lower evaporation of grain moisture. The heat transferred to the wet grain is a function of physical structure of the grain, temperature and moisture content of grains. The heat transferred to grain sets up internal temperature gradients within the grains and moisture transfer within the grain to the surface takes place by diffusion and capillary flow mechanisms. Towards the end of the process drying rate becomes steady and constant rate drying prevails. In the third phase the constant drying rate is attributed to progressive decrease in adsorptivity of desiccant beds.

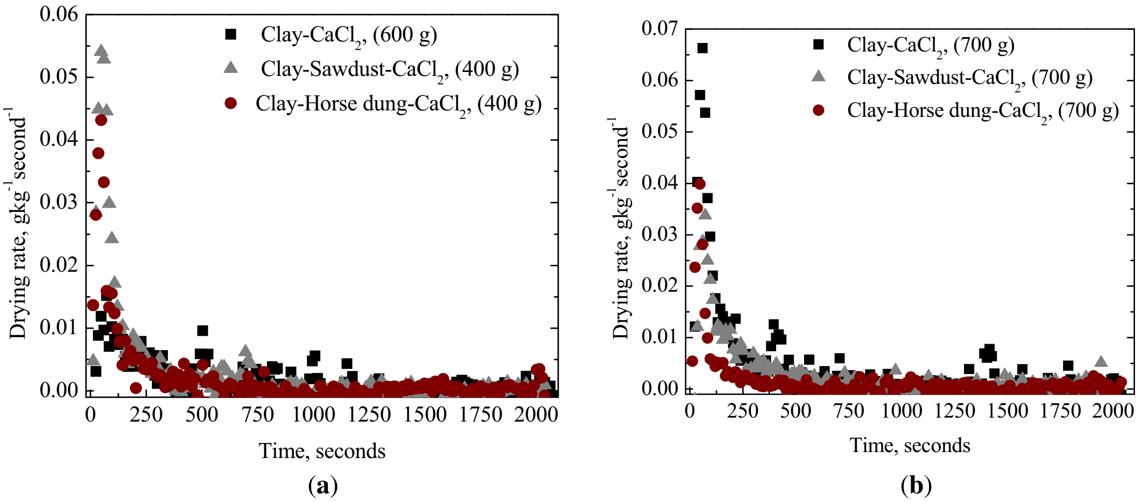

Figure 11. Variation of process air drying rate with respect to similar (a) D/L ratio and (b) desiccant bed masses.

The residual moisture content of grains is evaporated and carried by the circulating air. The drying rate curve presented reveals rapid transition from external drying stage to internal drying stage whereas the transition from external drying to constant rate drying is gradual.

3.2 *Overall moisture removed and characteristics of dried green pea grains*

The mass of green pea grains considered for drying is 250 g each contained on the bottom and top trays of the dryer. The initial weight of moist grains before drying and final weight of dried grains after drying is recorded for estimating the moisture removed during the elapsed drying period. The mass of water removed from the bottom and top tray grains are tabulated in table 2. The variation of total moisture removal rate with bed diameter to length (D/L) ratio is illustrated in figures 12(a) and (b). For the same bed masses of 500 g and 700 g the bed diameter to length ratio obtained is 0.21, 0.15 and 0.16, 0.10 for burnt clay-$CaCl_2$ and burnt clay-additives-$CaCl_2$ composite desiccant beds. With D/L ratio of 0.21 (500 g) and 0.16 (700 g) for clay-$CaCl_2$ vertical packed beds, the drying rates obtained are 0.44 g/min and 0.69 g/min. For D/L ratio of 0.15 (500 g) and 0.10 (700 g) of burnt clay-horse dung-$CaCl_2$ bed, the corresponding drying rates are 0.69 g/min and 0.81 g/min. With D/L ratio of 0.15 (500 g) and 0.10 (700 g) for burnt clay-sawdust-$CaCl_2$ vertical packed bed, the drying rates estimated are 0.63 g/min and 0.52 g/min.

The photographs of grains before drying and after drying are presented in figures 13(a) and (b). The visual examination of the grains shows the dehydrated surface of the grains after drying. The dehumidified surface indicates the removal of moisture from the grains. Change in color of grains is observed upon drying, but the change is minimal.

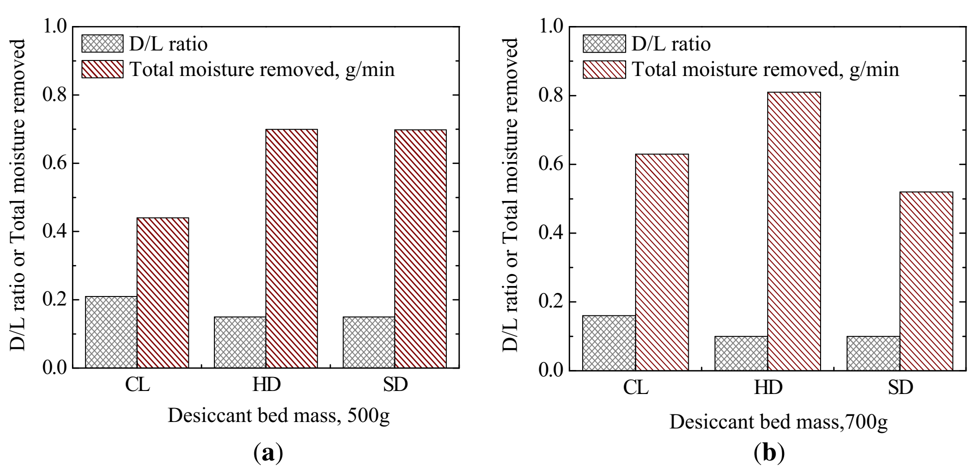

Figure 12. Overall moisture removed from the grain bed with respect to D/L ratio for (a) 500 g and (b) 700 g desiccant bed masses.

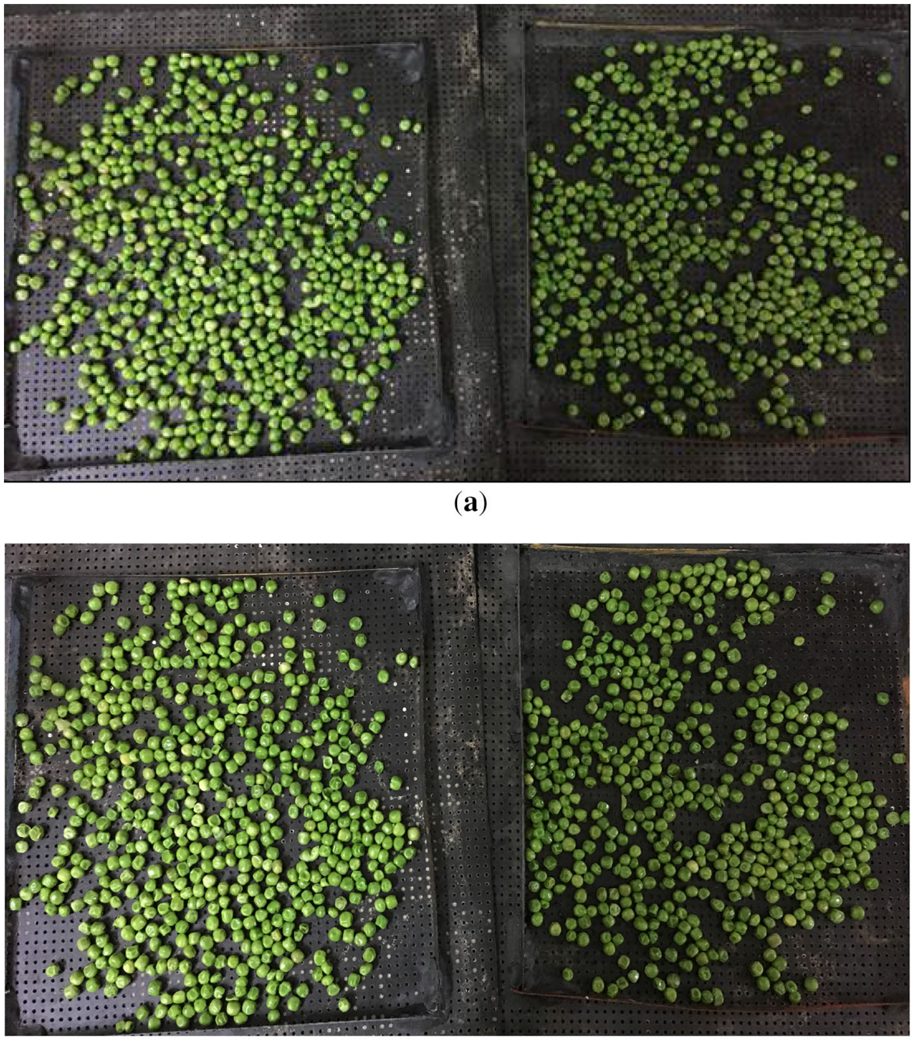

(**a**)

(**b**)

Figure 13. Photographs of green pea grains contained in the top and bottom trays of the dryer (a) before drying and (b) after drying.

Table 3. Texture characteristics of green pea grain images before and after drying.

Parameters	Before drying	After drying
Mean	Max:142.16, Min: 76.34	Max:149.59, Min: 89.12
Mode	Max:253, Min: 17	Max:231, Min: 14
Median	Max:145, Min: 62	Max:151, Min: 81
Standard deviation	47.57	52.01
Entropy	7.57	7.67
Energy	0.1431	0.1324
Contrast	0.1374	0.1343
Correlation	0.9697	0.9757
Homogeneity	0.9360	0.9389

The smaller change in color indicates the retainment of nutritional content even after drying. Further to quantify the characteristics of the investigation of the image was carried out by image processing. A code written in Matlab for image processing enables the estimation of texture features and statistical measures [26].

The parameters are estimated for the images before and after drying are tabulated in table 3. The percentage decrease in entropy which characterizes the randomness of the texture of the input image before drying and after drying is 1.30. The energy which measures the uniformity of the texture before drying is 0.1431 and 0.1324 after drying. The intensity of pixels is measured in terms of contrast. The difference in contrast values before drying and after drying is 0.005. The texture analysis of parameters yields a similarity index which is comparative value. The similarity index of 23.51 indicates the similarity of processed images as 77%. The image data in terms of statistical and texture parameters reveals a minimal change of color, shape and texture before and after drying. The smaller changes indicate the preservation of dietary and nutritional content of grains even after moisture removal.

4. Conclusions

The conclusions from the experimental study, involving the use of clay-based composite desiccants for drying of green peas are as follows:

1. For the identical conditions of temperature and humidity of process air the moisture uptake rate is higher for clay-additives based composite desiccants. For the same process time and process air conditions, attainment of saturation condition is at accelerated rate for clay-$CaCl_2$ composite desiccants.
2. Higher bed porosity prevailing in clay-additives-$CaCl_2$ composite desiccant beds lowers the pressure drop through the vertical packed heat-treated clay-additives-$CaCl_2$ composite desiccant beds as compared to clay-$CaCl_2$ composite desiccant bed.
3. For the identical desiccant bed masses and for the given volume of desiccant bed, the surface area available for moisture and heat transport is higher in additive based composite desiccants.
4. The maximum reduction in moisture from process air by the dry desiccant bed occurs within 500 s of process time. The corresponding moisture gain by process air from wet grains as compared to heat-treated clay desiccant beds, are higher for additives based desiccant beds.
5. The drying rate curve for process air reveals the presence of three drying stages namely surface drying (external drying), diffusion controlled drying (internal drying) and constant rate drying stage.
6. Image analysis of the green peas after subjecting to drying shows the potential of low-cost heat treated clay and clay-additives-$CaCl_2$ composite desiccants for agricultural and food products preservation, drying and aeration in humid climates.

Acknowledgements

This research work was carried out by research facilities provided at V. P. Dr. P. G. Halaktti College of Engineering and Technology Vijayapur, Karnataka state, India, The authors acknowledge the local pot makers of Vijayapur, for providing the clay material, horse dung and sawdust.

List of symbols

A_{sf} Surface area of desiccant bed (m^2)
d_p Diameter of spherical shaped desiccant (m)
dr Drying rate (g/kg s^{-1})
dt Time interval (s)
t_d Total process time (min)
Mr Overall moisture removed (g/min)
D Desiccant bed diameter (m)
G Reduction in grain mass (g)
h Enthalpy of humid air (kJ)
L Desiccant bed length (m)
m Moisture transferred (%)
W Air humidity ratio (g/kg)
w Mass of sample (g)
t Process time (s)
T Temperature (°C)
P Pressure (Pa)
V Volume (m^3)
v_s Superficial velocity (m/s)
X Manometer deflection (m)

Subscripts

a Air
b Desiccant bed
d Desiccant
i Inlet
e Exit
g Grain
v Vapor
sat Saturation

Greek letters

ρ Density (kg/m^3)
μ Viscosity (kg/ms)
ε Porosity (%)

Abbreviations

db Desiccant bed
gd Grain bed
RH Relative humidity
CL Clay
HD Horse dung
SD Sawdust

References

[1] Kumar D. and Kalita P. 2017 Reducing postharvest losses during storage of grain crops to strengthen food security in developing countries; *Foods* **6** 1–22
[2] Mujumdar A. S. and Law C. L. 2010 Drying technology: trends and applications in postharvest processing; *Food Bioprocess. Technol.* **3** 843–852

[3] Misha S., Mat S., Ruslan M. H. and Sopian K. 2012 Review of solid/liquid desiccant in the drying applications and its regeneration methods; *Renew. Sustain. Energy Rev.* **16** 4686–4707
[4] El-Sebaii A. A. and Shalaby S. M. 2013 Experimental investigation of an indirect-mode forced convection solar dryer for drying thymus and mint; *Energy Convers. Manag.* **74** 109–116
[5] Doymaz İ and Kocayigit F. 2011 Drying and rehydration behaviors of convection drying of green peas; *Dry. Technol.* **29** 1273–1282
[6] Dina S. F., Ambarita H., Farel H. N. and NapitupuluKawai F. H. H. 2015 Study on effectiveness of continuous solar dryer integrated with desiccant thermal storage for drying cocoa beans; *Case Stud. Therm. Eng.* **5** 32–40
[7] Mahdiyeh D., Mortezapour H., Akhavan H. R. and Moghaddam A. G. 2018 Tomato slices drying in a liquid desiccant-assisted solar dryer coupled with a photovoltaic-thermal regeneration system; *Sol. Energy* **162** 364–371
[8] Hanif S., Sultan M., Miyazaki T. and Koyama S. 2019 Investigation of energy-efficient solid desiccant system for wheat drying; *Int. J. Agric. Biol. Eng.* **12** 221–228
[9] Thoruwa T. F. N., Grant A. D., Smith J. E. and Johnstone C. M. 1998 A solar-regenerated desiccant dehumidifier for the aeration of stored grain in the humid tropics; *J. Agric. Eng. Res.* **71** 257–262
[10] Shanmugam V. and Natarajan E. 2006 Experimental investigation of forced convection and desiccant integrated solar dryer; *Renew. Energy* **31** 1239–1251
[11] Nagaya K., Li Y., Jin Z., Fukumuro M., Ando Y. and Akaishi A. 2006 Low-temperature desiccant-based food drying system with airflow and temperature control; *J. Food Eng.* **75** 71–77
[12] Hung B. N., Nuntaphan A. and Kiatsiriroat T. 2009 Integration of desiccant tray unit with internal cooling for aeration of paddy silo in humid tropical climate; *Biosyst. Eng.* **102** 75–82
[13] Hodali R. and Bougard J. 2001 Integration of a desiccant unit in crops solar drying installation: optimization by numerical simulation; *Energy Convers. Manag.* **42** 1543–1558
[14] Rajamani M., Mishra V. R. and Maliyekkal S. M. 2017 Bundled-firewood like AlOOH-$CaCl_2$ nanocomposite desiccant; *Chem. Eng. J.* **323** 171–179
[15] Mbuge D. O., Negrini R., Nyakundi L. O., Kuate S. P., Bandyopadhyay R., Muiru W. M. and Mezzenga R. 2016 Application of superabsorbent polymers (SAP) as desiccants to dry maize and reduce aflatoxin contamination; *J. Food Sci. Technol.* **53** 3157–3165
[16] Subramanyam N., Maiya M. P. and Murthy S. S. 2004 Application of desiccant wheel to control humidity in air-conditioning systems; *Appl. Therm. Eng.* **24** 2777–2788
[17] Kabeel A. E. 2009 Adsorption–desorption operations of multilayer desiccant packed bed for dehumidification applications; *Renew. Energy* **34** 255–265
[18] Srivastava N. S. and Eames I. W. 1988 A review of adsorbents and adsorbates in solid-vapour adsorption heat pump systems; *Appl. Therm. Eng.* **18** 707–714
[19] Hamed A. M. 2002 Theoretical and experimental study on the transient adsorption characteristics of a vertical packed porous bed; *Renew. Energy* **27** 525–541
[20] Hiremath C. R., Kadoli R. and Katti V. V. 2018 Experimental and theoretical study on dehumidification potential of clay-additives based $CaCl_2$ composite desiccants; *Appl. Therm. Eng.* **129** 70–83
[21] Robert J. M. 1988 Describing the uncertainties in experimental results; *Exp. Therm. Fluid Sci.* **1** 3–17
[22] Holman J. P. 1994 Experimental methods for engineers; 6th edn. McGraw-Hill Inc., New York
[23] Pesaran A. A. and Mills A. F. 1987 Moisture transport in silica gel packed beds-I. Theoretical study; *Int. J. Heat Mass Trans.* **30** 1037–1049
[24] Hamed A. M., Abd-Elrahman W. R., El-Emam S. H. and Awad M. M. 2013 Theoretical and experimental investigation on the transient coupled heat and mass transfer in a radial flow desiccant packed bed; *Energy Convers. Manag.* **65** 262–271
[25] Qiongfen Y., Xiaolong T., Honghong Y., Ping N., Liping Y., Lina Y., Lili Y. and Hua L. 2009 Equillibrium and heat of adsorption of phosphine on CaCl2-modified molecular sieve. *J. Chem. Eng.* **4** 612–617
[26] Ganesh C. B., Pathak R., Ahmadi M. and Mistry P. 2018 Image processing analysis to track colour changes on apple and correlate to moisture content in drying stages; *Food Qual. Saf.* **0** 1–6